



Published in final edited form as:

Ann Neurol. 2017 April ; 81(4): 560–571. doi:10.1002/ana.24907.

***Olig1* is required for Noggin-induced neonatal myelin repair**

Jennifer K. Sabo, Ph.D.^{1,#}, Vivi Heine, Ph.D.^{1,†}, John C. Silbereis, Ph.D.^{2,^}, Lucas Schirmer, M.D.^{3,4}, Steven W. Levison, Ph.D.⁵, and David H. Rowitch, M.D., Ph.D.^{1,6,*}

¹Department of Pediatrics, Eli and Edythe Broad Center for Stem Cell Research and Regeneration Medicine, University of California, San Francisco, San Francisco, CA 94143, USA

²Department of Neuroscience, University of California San Francisco, San Francisco, CA, 94143, USA ³Eli and Edythe Broad Center for Stem Cell Research and Regeneration Medicine,

University of California, San Francisco, San Francisco, CA 94143, USA ⁴Department of

Neurology, Klinikum rechts der Isar, Technical University of Munich, 81675 Munich, Germany

⁵Department of Neurology and Neuroscience, New Jersey Medical School, Rutgers University-New Jersey Medical School, Newark, New Jersey 07103, USA ⁶Department of Paediatrics,

Wellcome Trust-MRC Stem Cell Institute, Cambridge University, Cambridge CB2 0QQ UK

[#]California Institute for Quantitative Biosciences, University of California, Berkeley, Berkeley, CA

94720, USA [†]Center for Children with White Matter Disorders, Center for Neurogenomics and

Cognitive Research, Department of Pediatrics, VU University Medical Center, 1081 HV

Amsterdam, Netherlands [^]Department of Neuroscience, Yale University, New Haven, CT 06520,

USA

Abstract

Objective—Neonatal white matter injury (NWMI) is a lesion found in preterm infants that can lead to cerebral palsy. Although antagonists of bone morphogenetic protein (BMP) signaling, such as Noggin, promote oligodendrocyte precursor cell (OPC) production after hypoxic-ischemic injury, the downstream functional targets are poorly understood. The bHLH protein *Olig1* promotes oligodendrocyte (OL) development and is essential during remyelination in adult mice. Here, we investigated whether *Olig1* function is required downstream of BMP antagonism for the response to injury in the neonatal brain.

Methods—We used wild type and *Olig1* mutant mice subjected to neonatal stroke and postnatal neural progenitor cultures, and we analyzed *Olig1* expression in human postmortem samples from neonates that suffered hypoxic-ischemic encephalopathy (HIE).

Results—*Olig1*-null neonatal mice showed significant hypomyelination after moderate neonatal stroke. Surprisingly, damaged white matter tracts in *Olig1*^{-/-} mice lacked *Olig2*⁺ OPCs and

* Address correspondence to David H. Rowitch, M.D., Ph.D., 35 Medical Center Way, San Francisco, CA 94143. Phone: (415) 476-7242, david.rowitch@ucsf.edu.

Author contributions

J.K.S., V.H., J.C.S. and L.S. acquired and analyzed the data.

J.K.S., V.H., J.C.S., S.W.L. and D.H.R. designed the experiments.

J.K.S. and D.H.R. wrote the manuscript.

Potential Conflicts of Interest

Nothing to report.

instead proliferating neuronal precursors and GABAergic interneurons were present. We demonstrate that Noggin-induced OPC production requires *Olig1* function. In postnatal neural progenitors, Noggin governs production of OLs versus interneurons through *Olig1*-mediated repression of *Dlx1/2* transcription factors. Additionally, we observed that *Olig1* and the BMP signaling effector pSMAD1/5/8 are elevated in the subventricular zone (SVZ) of human infants with HIE compared to controls.

Interpretation—These findings indicate that *Olig1* has a critical function in the regulation of the postnatal neural progenitor cell production in response to Noggin.

INTRODUCTION

Human neonatal white matter injury (NWMI) is a complication observed in very low and extremely low birth weight preterm infants. NWMI has been associated with development of cerebral palsy (CP), a lifelong condition with variable motor features including chronic spastic paraplegia and dysarthria^{1–2}. Neuroimaging and pathological studies have highlighted changes in the nature of lesions of NWMI over the past few decades. While focal cystic necrotic lesions (aka, periventricular leukomalacia) were characteristic pathological hallmarks in the 1980's, it is now more common to find diffuse non-cystic white matter injury³. The oligodendrocyte (OL) is the myelinating cell of the central nervous system (CNS) and has long been considered a cellular target in NWMI. Pathological studies provide evidence for arrest of oligodendrocyte precursor cell (OPC) maturation in NWMI, which is predicted to lead to a failure in myelination of white matter tracts^{4,5,6}. We have shown that OPCs in such lesions express markers of Wnt signaling, a pathway that can cause OPC maturation arrest^{7,8,9}.

In this study, we investigated the function of the bHLH protein *Olig1* in hypoxic-ischemic (HI) neonatal diffuse gliotic WMI. *Olig1* and *Olig2* have critical roles in OPC specification, maturation and myelination, and *Olig1* is essential for establishment of OPCs from the ventral forebrain^{10,11}. In the embryonic forebrain, *Olig1* regulates cell fate choice between interneuron and OPC specification¹¹, and mice lacking *Olig1* function show exaggerated production of calretinin and parvalbumin positive interneurons at the expense of OPCs. Might these mechanisms also have relevance in progenitor cell responses to white matter injuries in the postnatal period? Bone morphogenetic proteins (BMPs) are secreted growth factors that are expressed in OPCs and OLs derived from the CNS¹². The BMP pathway is activated upon ligand/receptor formation, and phosphorylation of the intracellular SMAD1/5/8 protein complex is increased with each SMAD forming a heteromeric receptor complex with SMAD4¹³. Mice lacking BMP receptor, BMPRIa in *Olig1*-expressing progenitors show increased numbers of oligodendroglia and interneurons in the brain at birth¹⁴. Prior work shows that repair of white matter injury requires the presence of OPCs recruited either from the local parenchyma or the subventricular zone (SVZ)^{15–18}, and that the BMP antagonist Noggin promotes OPC production in the setting of such injuries^{19–20}.

Previous studies show that *Olig1* function is required for OPC differentiation in adult white matter injury²¹, and that *Olig1* is upregulated in the neonatal SVZ after HI injury²². Here, we asked whether *Olig1* was required for repair after neonatal brain injury, and more

specifically whether Noggin –induced oligodendroglialogenesis requires *Olig1*. We subjected wild type and *Olig1*-null animals to a standard model of neonatal stroke, and observed a deficit of OPCs in the cerebral white matter. Surprisingly, we identified a large number of interneurons in the white matter. *Olig1*-null neuroepithelial cultures failed to produce OPCs in response to Noggin. Thus, *Olig1* function is critical for the Noggin-induced production of OPCs *in vitro* and myelination post-injury *in vivo*. Upregulation of *Olig1* and activated BMP signaling proteins in human cases of neonatal HIE suggests clinical relevance of this mechanism.

SUBJECTS/MATERIALS AND METHODS

Animals

All animal protocols were approved by the Institutional Animal Care and Use Committee at the University of California San Francisco (UCSF), CA, Dana-Farber Cancer Institute, Boston, MA and New Jersey Medical School, Newark, NJ. All animal studies were conducted in accordance with the United States Public Health Service’s Policy on Humane Care and Use of Laboratory Animals. Mouse colonies were maintained in accordance with institutional guidelines. C57BL/6 mouse colonies were established from mice initially purchased from Taconic Biosciences. The *Olig1*^{-/-} mice have been previously described^{10–11}.

Mouse neonatal hypoxia-ischemia (HI)

Mouse pups were delivered normally with the day of birth considered as postnatal day 0 (P0). For a term stroke model, which encompasses white matter injury, cerebral HI was induced in P9 pups by right common carotid artery (RCCA) cauterization followed by systemic hypoxia. Briefly, pups were lightly anesthetized with isoflurane (4% induction, 3% maintenance). Once fully anesthetized, a midline neck incision was made and the CCA was identified. The CCA was separated from the vagus nerve and then cauterized using a bipolar cauterizer at power setting of 10. Animals were returned to the dam for 1.5 h. Before exposure to hypoxia in humidified gas (10% O₂/90% N₂), the pups were pre-warmed in jars for 20 min in a 37°C water bath. The pups were then exposed to 65 min of hypoxia at 36°C. After hypoxia, the pups were allowed to recover in the jars for 20 min and were then returned to the dam for recovery periods of 2–4 wks, at which point they were anesthetized and intracardially perfused with cold 4% paraformaldehyde (PFA) in 0.1 M phosphate buffered saline (PBS), pH 7.4. Brains were postfixed in the same solution and cryopreserved in 30% sucrose in 0.1M PBS. For bromodeoxyuridine (BrdU) incorporation studies one-week post HI, wild type and *Olig1*^{-/-} pups were given daily intraperitoneal injections of BrdU (50 mg/kg) from P14–P16. All BrdU injected mice were euthanized at P23. We scored “mild brain injury” as no detectable loss of volume on the ipsilateral side, “moderate brain injury” as preservation greater than 2/3 volume of ipsilateral versus contralateral hemisphere and “severe brain injury” loss of greater than 2/3 volume of ipsilateral versus contralateral hemisphere.

Human developmental tissue

All human tissue was collected in accordance with guidelines established by the UCSF Committee on Human Research (H11170-19113-07). Immediately after autopsy, all brains were immersed in PBS with 4% PFA for 3 days. On day 3, the brain was cut in the coronal plane at the level of the mammillary body and immersed in fresh 4% PFA/PBS for additional 3 days. Post fixation, all tissue samples were equilibrated in PBS with 30% sucrose for 2 days, allowing the samples to reach optimum cutting temperature medium embedding. The diagnosis of HIE requires clinical and pathological correlations. With respect to the pathological features, all HIE cases showed consistent evidence of diffuse white matter injury, including astrogliosis and macrophage activation. These findings were confirmed by an increase in the number of and staining intensity of GFAP- or CD68-positive cells, respectively. In addition, the HIE cases also showed evidence of neuronal injury, including the presence of ischemic neurons and variable degrees of neuronal loss, in cerebral cortex, hippocampus and basal ganglia. Three cases of HIE and four cases of controls were analyzed (see Table I). Cases 1–3 demonstrated clinical and pathological evidence of HIE and low output state in multiple organs on post-mortem examination. Specific findings in case 1 (2 months old, born at full term) included hypoplastic left heart and diffuse WMI in brain with focal neuron dropout in cerebral and cerebellar cortices. Case 2 (5 months old, born prematurely at 26 weeks gestation) had a clinical diagnosis of severe HIE and underwent therapeutic hypothermia, showed diffuse white matter injury on postmortem evaluation. Case 3 was 6 days old born at 37 weeks and 4 days. Cases 4–7 were controls, with the following age and gestational age information: case 4 was 7 months old born at 31 weeks, case 5 was 2 days old born at 37 weeks and 3 days, case 6 was born at 36 weeks and 4 days and case 7 was 11 days old born at 37 weeks and 6 days. The SVZ was the area examined in all cases.

Immunohistochemistry (IHC) in human and mouse samples

IHC was performed on 16 μ m serial sections with blocking and antibody incubation carried out overnight at 4°C in PBS containing 0.3% Triton/10% normal goat serum with the exception of GAD67 for which Triton was excluded. For human brains, the cryosections were heated for antigen retrieval in sodium citrate buffer before blocking. Primary antibodies were used at the following dilutions: rabbit Olig2 (1:2000; Dr. Charles D Stiles, Dana Farber Cancer Institute; Boston MA), rabbit Olig1 (1:1000; Dr. Charles D Stiles, Dana Farber Cancer Institute; Boston MA), mouse MBP (1:1000; Covance), rabbit DCX (1:500; Cell Signaling); mouse BrdU (1:100; BD Biosciences); mouse GAD67 (1:500; Millipore); mouse Tuj1 (1:1000; Covance); rabbit GFAP (1:1000; Dako); rat PDGFR α (1:500 BD Biosciences), rabbit pSMAD1/5/8 (1:1000; Cell Signaling). BrdU detection was carried out as previously described¹⁸, with IHC for the protein of interest carried out as described above before the application of the BrdU antibody. After primary antibody incubation and washes, sections were incubated with Alexa-fluor conjugated species directed secondary antibodies (Invitrogen) and then rinsed before being mounted with DAPI Fluoromount-G.

Cell Culture

Postnatal neurospheres and monolayer cultures were established from P7 microdissected subventricular zone from wild type and *Olig1*-null animals and grown in DMEM/F12 (Invitrogen) supplemented with penicillin/streptavidin, N2, B27, EGF and bFGF (20 ng/mL each). Cells were passaged once a week which involved disassociating with Trypsin (Life Technologies) followed by mechanical trituration. According to the experimental paradigm, cells were either cultured in the presence or absence of BMP4 (10ng/mL; R&D systems) and Noggin (250ng/mL; R&D systems). Cells were differentiated by removing EGF and bFGF from the medium before being cultured for an additional week. For immunocytochemistry of neural stem cell cultures, cells were allowed to differentiate on BD biocoat poly-D-lysine/laminin coated coverslips as described above and fixed for 10 min in 4% PFA. Blocking was carried out in PBS containing 0.1% Triton/5% normal goat serum with the exception of GABA and O4 for which Triton was excluded. Antibody incubation was carried out overnight at 4°C in PBS containing 5% normal goat serum. Primary antibodies were used at the following dilutions: mouse Olig2 (1:500), rabbit GABA (1:1000; Sigma), rabbit DCX (1:500); mouse GalC (1:500; Millipore); mouse Nkx2.2 (1:250; DSHB); mouse IgM O4 (1:100; Dr. Rashmi Bansal, University of Connecticut; Farmington CT). Washing steps and secondary antibody incubation were carried out as described above and coverslips were mounted onto slides using DAPI Fluoromount-G (SouthernBiotech).

Image acquisition and cell counts

Confocal images were obtained using a Leica SPE upright microscope with the 40x objective, whereas fluorescent images were obtained using a Nikon 80i or Zeiss Axioskop2 with the 20x objective. For IHC cell counts in mouse tissue, at least three animals per genotype were used and cells were counted on three or more non-adjacent sections. Likewise, for human tissue, there were at least three cases per condition and cells in the dorsolateral SVZ were counted on two non-adjacent sections. The borders of the dorsolateral SVZ were outlined using a drawing tool, and the areas were measured using Adobe Photoshop with the data being expressed as mean value/mm² ± SEM. For ICC cell counts, cells were quantified at two defined locations at the edge of each coverslip.

Quantitative PCR

Total RNA was isolated from wild type cells in culture using Trizol reagent (Invitrogen) and then cleaned up with RNeasy Mini Kit (Qiagen). The cDNA was made using the High Capacity RNA to cDNA Master Mix (Applied Biosystems). All qPCR was performed using SYBR Green master mix on a Roche Lightcycler 480. The relative expression from RNA samples was determined using the 2^{-CT} method. Values were normalized to the expression of the beta-actin housekeeping gene. Primers were designed using Primer3, and the sequences are as follows: Olig1: forward- GCTGCGCGAAGTTATCCTAC, reverse – ACCCAGCAGCAGGATGTAGT; Dlx2: forward – CTGGCCTCAATTCCGACCT, reverse – GGCCTGAAGAGACCAAGGAC; Dlx1: forward – TTCCGTTCTGTTGTGTGTGG, reverse – GGTGGATTTCAATCGGTAC; Noggin: forward – GGTGTGTAAGCCATCCAAGTCT, reverse – CCGAGTTCTAGCAGGAACACTTAC;

Olig2: forward – GAAGCAGATGACTGAGCCCGAG, reverse –
CCCGTAGATCTCGCTCACCAG.

Western Blot

Total cell lysate was collected from wild type and *Olig1*-null cells in RIPA buffer (Pierce) supplemented with proteinase and phosphatase inhibitor cocktails (Roche), resolved by SDS-Page and immunoblotted using standard techniques with the antibodies described above in addition to mouse beta-actin antibody (Sigma). Band intensity was measured using ImageJ software (NIH).

Statistical Analyses

For all cell counts, statistical tests were performed using GraphPad Prism. One-way ANOVA with Dunnett's multiple comparison test was used for comparison between groups, and Student's unpaired *t* test was used for two group comparisons. All cell counts and analyses were performed blind to experimental treatment. Data are expressed as mean \pm SEM.

RESULTS

***Olig1* is neuroprotective and regulates OPC versus interneuron production following neonatal stroke**

To investigate *Olig1* function in the injury response, we subjected *Olig1*-null and wild type animals to neonatal stroke²³ (Figure 1A–B). BrdU was administered one-week post injury and animals were sacrificed two or four weeks post injury (Figure 2B). This procedure results in a variable extent of brain injury (Figure 1A, 2A). We selected only brains that had mild or moderate brain injury ipsilateral to the manipulated hemisphere (defined by the appearance of small cysts and/or ventriculomegaly with astrogliosis in the affected hemisphere) for analysis. Severely injured samples (defined as near-total ipsilateral hemispheric loss) were ruled out. At two- and four-weeks post injury *Olig1*^{-/-} consistently showed increased brain injury compared to wild type controls (Figure 1C, D). After two- and four-weeks following injury, *Olig1*-null animals were more poorly myelinated compared to controls (Figure 1G–H, K–L), despite the presence of intact axons (Figure 1I–J). Indeed, we found surprising abnormalities in the ratios of neuron and glial precursor populations. First, populations of Olig2- (Figure G–H, M) and PDGFR α -labeled OPCs (Figure M) were greatly reduced in the corpus callosum of the *Olig1*-null animals two weeks and four weeks post injury. This was associated with significantly ($p = 0.01$) decreased proliferation of Olig2-positive cells in *Olig1*-null animals compared to wild type (Figure 2C–D, F). We did not find the overall number of proliferating cells to be altered (BrdU+: wild type: 155 ± 42.7 ; *Olig1*-null: 181 ± 14.8 ; $p = 0.59$). Second, we asked whether the deficient population of OPC cells might relate to dysfunction in OPC specification, similar to what has been observed in the *Olig1*^{-/-} embryonic forebrain. Indeed, we observed a corresponding significant ($p = 0.01$) increase in the number of proliferating DCX-positive cells in the subcortical white matter of *Olig1*-null animals (Figure 2C, D, F). In *Olig1*-null animals, DCX-positive cells colocalized with the neuron-specific marker Tuj1 and the GABAergic interneuron protein GAD67 but not with Olig2 (data not shown) (Figure 2E). We never observed DCX/GAD67 co-labeled cells in the white matter of wild type animals. These findings indicate that *Olig1*

function is required to regulate OL production in postnatal forebrain after HI injury. In the absence of *Olig1*, neural precursors adopt an interneuron fate, which then invade the cerebral white matter.

Noggin-induced OPC production requires *Olig1*

Injury to white matter tracts can stimulate SVZ cells to increase the production of neural progenitors for repair^{15, 17, 24–25}. In the setting of such injuries, the BMP antagonist Noggin is an inducer of the oligodendrogenic response of neural precursor cells^{19–20}. We assessed *Olig1* and *Noggin* expression in the SVZ of wild type animals seven days after HI injury and found elevated mRNA levels for *Olig1* and *Noggin* in injured animals compared to sham controls (data not shown). Noggin can promote production of OLs^{12,19,26}. To determine a role for *Olig1* downstream of Noggin, we generated both neurospheres and adherent cultures of neural stem cells (NSC) from P7 dorsal SVZ of wild type and *Olig1*-null animals in a biochemically defined medium or medium supplemented with BMP4 (10ng/mL), Noggin (250ng/mL) or BMP4+Noggin (10ng/mL and 250ng/mL). In wild type NSC adherent cultures expanded in EGF and FGF and supplemented with Noggin, both *Olig1* mRNA and protein were induced after six hours (Figure 3A,B). To investigate Noggin-induced programs of differentiation, we transferred wild type and *Olig1*-null adherent cultures to growth factor-free media for seven days. As shown (Figure 3C–D), *Olig1*-null cultures produced significantly fewer OPCs and immature OLs (Nkx2.2+ and O4+) and fewer mature OLs (GalC+) at baseline compared to wild type. While addition of Noggin to wild type cultures significantly expanded the counts of OL lineage cells, *Olig1*-null cultures failed to respond to Noggin treatment. In keeping with this, qPCR and Western blot analyses of *Olig1*-null cultures treated with Noggin showed decreased expression of OL markers compared to wild type cultures (Figure 3E–G). These data indicate that *Olig1* is required for the Noggin-induced production of OLs from neural precursors.

Noggin treatment represses *Dlx1/2* in an *Olig1*-dependent manner

Given the observation that *Olig1* represses embryonic interneuron production by inhibiting *Dlx1/2* expression¹¹, one possibility was that Noggin-induced OPC production from neuroprogenitors involved *Olig1*-mediated repression of *Dlx1* and/or *Dlx2*. We therefore assessed Noggin-treated *Olig1*-null cultures for their ability to produce interneurons monolayer cultures. *Olig1*-null neurospheres, both in the presence and absence of Noggin produced more DCX-positive immature neurons (which did not co-label with Olig2) and fewer Olig2-positive cells (Figure 4A–B). There was a trend in *Olig1*-null monolayer cultures treated with Noggin to produce fewer GABAergic interneurons, however this condition was not significant. We next tested whether BMP signaling regulates the interneuron versus OL fate choice through *Dlx1* and/or *Dlx2*. Indeed, *Olig1*-null mutants show increased expansion of *Dlx1* and *Dlx2* expression in the embryonic brain¹¹. As shown (Figure 4C), qPCR analysis of wild type adherent cultures treated with BMP4, Noggin or BMP4+Noggin showed that BMP4 induced upregulation of *Dlx1*, *Dlx2* transcript levels while reducing mRNA for *Olig2*. Taken together, these findings suggest that *Olig1* function mediates Noggin-induced repression of *Dlx1/2* in adherent neuroepithelial cultures (Figure 4D).

Evidence for Olig1 upregulation and BMP pathway activation in human neonatal SVZ progenitors following hypoxic-ischemic injury

To assess the relevance of these findings to human brain injury, we first investigated the expression of Olig1 proteins in the dorsolateral SVZ of term human neonate HIE cases and controls (Figure 5). As shown (Figure 5B–C, H) we observed increased numbers of Olig1-positive cells (and similar DCX expression) in HIE cases compared to controls (DCX-positive cells: control: 1286 ± 168.2 ; HIE: 1881 ± 334.5 ; $p=0.16$). Furthermore, BMP signaling was activated in HIE as evidenced by pSMAD1/5/8 immunostaining (Figure 5D–E). In control and HIE cases, Olig1 co-localized with pSMAD1/5/8 in SVZ progenitors (Figure 5F–G). Quantification revealed significantly ($p=0.004$) increased numbers of pSMAD1/5/8+/Olig1+ cells in the SVZ of HIE cases, with Olig1 expressed in the majority of pSMAD1/5/8+ cells (Figure 5H). These findings confirm that Olig1 and BMP signaling become upregulated in human neonatal neural precursors in cases of HIE, supporting the possibility that BMP signaling could inhibit the maturation of Olig1 cells in the SVZ post-injury and that by extension highlight why Noggin signaling could have an important role to promote effective OPC production.

DISCUSSION

It is important to identify the underlying mechanisms and new therapeutic targets for NWML. In this study, we interrogated the function of the OL transcription factor, *Olig1*, in HI neonatal diffuse gliotic white matter injury. Our results show that *Olig1* is a potent regulator of GABAergic interneuron versus OL cell fate acquisition in the injured white matter. They demonstrate that *Olig1* is required for OL production and myelin generation in the context of neonatal white matter injury, and that *Olig1* functions downstream of Noggin signaling to promote postnatal production of OPCs.

Olig1 regulation during development and after injury

Early *Olig1* expression in the ventral telencephalon *in vivo* and in embryonic neural progenitors *in vitro* is regulated by Sonic hedgehog (Shh)^{11,27}, suggesting that Shh initially induces *Olig1* and patterns the embryonic septum and medial ganglionic eminence. Noggin also participates in early neural patterning events by antagonizing BMPs and working synergistically with Shh to promote ventral cell fates²⁸. BMP treatment of embryonic mouse ventral neuroepithelial explants inhibits Shh induced oligodendroglialogenesis, but fails to fully inhibit this process once it has already been initiated at E6, indicating a role for BMP in early cell fate specification²⁹. At later stages and in the setting of neonatal brain injury where BMP expression is increased³⁰, BMP antagonists have been proposed to increase production of OLs^{17, 31–32}. We find that Noggin strongly induces Olig1 in neuroepithelial cultures, and that in the absence of *Olig1* function Noggin fails to induce OPCs, demonstrating an essential downstream role in multipotent progenitors *in vitro*.

Olig1 regulates OPC versus interneuron production in postnatal neural progenitors after hypoxic-ischemic insult

An unexpected finding was that ectopic DCX-positive immature neurons were present in the white matter tracts of *Olig1*^{−/−} animals after neonatal HI brain injury. These ectopic DCX

cells were *bona fide* interneurons as they co-expressed GAD67+ but not Olig2. While the white matter has a large number of these interneurons, it is not clear whether findings in *Olig1*-null mice are due to aberrant migration of progenitors into the white matter or expansion of rare resident progenitors that differentiate into interneurons. Future work will be needed to show the origin of the cells and whether they fully differentiate. Our *in vitro* data show increased production of GABAergic interneurons in *Olig1*-null progenitors at baseline, which is reminiscent of *Olig1*'s role to regulate interneuron versus OPC fate in the embryonic telencephalon. In the embryo, *Olig1* represses the domain of *Dlx1/2* expression to preserve a progenitor cohort for later wave OPC production¹¹. The situation in the postnatal SVZ and in progenitors in culture is obviously spatio-temporally quite different. Nevertheless, *Olig1* exerts a similar role in both contexts to repress *Dlx1/2* and promote OPC production at the expense of interneurons. As an aside, this finding could be exploited for production of interneurons, e.g., to inhibit seizure activity in animal models³³, as *Olig1*-/- neural progenitors overproduce interneurons.

***Olig1* functions downstream of BMP signaling inhibition by Noggin to promote OPC production after hypoxic-ischemic injury**

The response to brain injury provides another instance of regulation of neurogenesis in the SVZ progenitors. For instance, subsequent to focal toxic damage to white matter with lysolethicin, SVZ progenitors are activated to produce OPCs versus neurons¹⁶, through activity of Noggin^{19, 26}. These studies highlight the regenerative capacity of SVZ progenitors particularly in adult white matter injury. Prior studies have shown that the SVZ expands after neonatal HI injury^{15, 22, 34–35} and that *Olig1* transcript levels are elevated following HI²². Indeed, in the human neonate with HIE we found elevated numbers of *Olig1*-positive cells compared to controls. Moreover, consistent with a role for BMP signaling regulation, the majority of the *Olig1*-positive cells co-expressed pSMAD1/5/8. Further work is needed to determine whether BMP signaling in *Olig1*-positive progenitors would block or delay OPC maturation in the setting of HIE, but findings from this and other studies suggests the importance of the BMP antagonism by Noggin or similar agents to promote OPC production in stroke³², perinatal HI³⁶, perinatal intraventricular hemorrhage³⁷, intrauterine growth retardation³⁸ and myelin deficient animals³⁹. Our model is one of term neonatal stroke, and further work is needed to show a role for *Olig1* in other models of preterm NWMI. However, these studies suggest benefit of Noggin and *Olig1* activities in neonatal brain injury.

Acknowledgments

The authors thank Vien Nguyen, Sandra Chang and Khalida Sabeur for expert technical help. J.S. gratefully acknowledges support from UCSF T32 training grant (JS; T32CA151022). L.S. was supported by a postdoctoral fellowship from the German Research Foundation (DFG, SCHI 1330/1-1). This work has been supported by Howard Hughes Medical Institute and grants from NINDS to D.H.R. (NS040511 and P01NS083513) and NIH to S.W.L. (R01 HD052064).

References

1. Nelson KB, Lynch JK. Stroke in newborn infants. *Lancet Neurol.* 2004; 3:150–1588. [PubMed: 14980530]

2. Woodward LJ, Anderson PJ, Austin NC, et al. Neonatal MRI to predict neurodevelopmental outcomes in preterm infants. *N Engl J Med*. 2006; 355:685–694. [PubMed: 16914704]
3. Back SA. Perinatal white matter injury: The changing spectrum of pathology and emerging insights into pathogenetic mechanisms. *Ment Retard Dev Disabil Res Rev*. 2006; 12:129–140. [PubMed: 16807910]
4. Billiards SS, Haynes RL, Folkerth RD, et al. Myelin abnormalities without oligodendrocyte loss in periventricular leukomalacia. *Brain Pathol*. 2008; 18:153–163. [PubMed: 18177464]
5. Segovia KN, McClure M, Moravec M, et al. Arrested oligodendrocyte lineage maturation in chronic perinatal white matter injury. *Ann Neurol*. 2008; 63:520–530. [PubMed: 18393269]
6. Buser JR, Maire J, Riddle A, et al. Arrested preoligodendrocyte maturation contributes to myelination failure in premature infants. *Ann Neurol*. 2012; 71:93–109. [PubMed: 22275256]
7. Fancy SP, Baranzini SE, Zhao C, et al. Dysregulation of the Wnt pathway inhibits timely myelination and remyelination in the mammalian CNS. *Genes Dev*. 2009; 23:1571–85. [PubMed: 19515974]
8. Fancy SP, Harrington EP, Yuen TJ, et al. Axin2 as regulatory and therapeutic target in newborn brain injury and remyelination. *Nat Neurosci*. 2011; 14:1009–16. [PubMed: 21706018]
9. Fancy SP, Harrington EP, Baranzini SE, et al. Parallel states of pathological Wnt signaling in neonatal brain injury and colon cancer. *Nat Neurosci*. 2014; 17:506–12. [PubMed: 24609463]
10. Lu QR, Sun T, Zhu Z, et al. Common developmental requirement for Olig function indicates a motor neuron/oligodendrocyte connection. *Cell*. 2002; 109:75–86. [PubMed: 11955448]
11. Silbereis JC, Nobuta H, Tsai HH, et al. Olig1 function is required to repress *dlx1/2* and interneuron production in mammalian brain. *Neuron*. 2014; 81:574–587. [PubMed: 24507192]
12. Kondo T, Raff M. A role for Noggin in the development of oligodendrocyte precursor cells. *Dev Biol*. 2004; 267:242–251. [PubMed: 14975730]
13. Massagué J. TGF-beta signal transduction. *Annu Rev Biochem*. 1998; 67:753–791. [PubMed: 9759503]
14. Samanta J, Burke GM, McGuire T, et al. BMPRIa signaling determines numbers of oligodendrocytes and calbindin-expressing interneurons in the cortex. *J Neurosci*. 2007; 27:7397–7407. [PubMed: 17626200]
15. Yang Z, Levison SW. Hypoxia/ischemia expands the regenerative capacity of progenitors in the perinatal subventricular zone. *Neuroscience*. 2006; 139:555–564. [PubMed: 16500031]
16. Menn B, Garcia-Verdugo JM, Yaschine C, et al. Origin of oligodendrocytes in the subventricular zone of the adult brain. *J Neurosci*. 2006; 26:7907–7918. [PubMed: 16870736]
17. Jablonska B, Aguirre A, Raymond M, et al. Chordin-induced lineage plasticity of adult SVZ neuroblasts after demyelination. *Nat Neurosci*. 2010; 13:541–550. [PubMed: 20418875]
18. Xing YL, Roth PT, Stratton JA, et al. Adult neural precursor cells from the subventricular zone contribute significantly to oligodendrocyte regeneration and remyelination. *J Neurosci*. 2014; 34:14128–14146. [PubMed: 25319708]
19. Cate HS, Sabo JK, Merlo D, et al. Modulation of bone morphogenic protein signalling alters numbers of astrocytes and oligodendroglia in the subventricular zone during cuprizone-induced demyelination. *J Neurochem*. 2010; 115:11–22. [PubMed: 20193041]
20. Sabo JK, Aumann TD, Merlo D, et al. Remyelination is altered by bone morphogenic protein signaling in demyelinated lesions. *J Neurosci*. 2011; 31:4504–4510. [PubMed: 21430151]
21. Arnett HA, Fancy SP, Alberta JA, et al. bHLH transcription factor Olig1 is required to repair demyelinated lesions in the CNS. *Science*. 2004; 306:2111–2115. [PubMed: 15604411]
22. Felling RJ, Snyder MJ, Romanko MJ, et al. Neural stem/progenitor cells participate in the regenerative response to perinatal hypoxia/ischemia. *J Neurosci*. 2006; 26:4359–69. [PubMed: 16624956]
23. Brazel CY, Rosti RT, Boyce S, et al. Perinatal hypoxia/ischemia damages and depletes progenitors from the mouse subventricular zone. *Dev Neurosci*. 2004; 26:266–274. [PubMed: 15711066]
24. Yang Z, Covey MV, Bitel CL, et al. Sustained neocortical neurogenesis after neonatal hypoxic/ischemic injury. *Ann Neurol*. 2007; 61:199–208. [PubMed: 17286251]

25. Yang Z, You Y, Levison SW. Neonatal hypoxic/ischemic brain injury induces production of calretinin-expressing interneurons in the striatum. *J Comp Neurol*. 2008; 511:19–33. [PubMed: 18720478]
26. Colak D, Mori T, Brill MS, et al. Adult neurogenesis requires Smad4-mediated bone morphogenetic protein signaling in stem cells. *J Neurosci*. 2008; 28:434–446. [PubMed: 18184786]
27. Lu QR, Yuk D, Alberta JA, et al. Sonic hedgehog-regulated oligodendrocyte lineage gene encoding bHLH proteins in the mammalian central nervous system. *Neuron*. 2000; 25:317–329. [PubMed: 10719888]
28. McMahon JA, Takada S, Zimmerman LB, et al. Noggin-mediated antagonism of BMP signaling is required for growth and patterning of the neural tube and somite. *Genes Dev*. 1998; 12:1438–1452. [PubMed: 9585504]
29. Mekki-Dauriac S, Agius E, Kan P, et al. Bone morphogenetic proteins negatively control oligodendrocyte precursor specification in the chick spinal cord. *Development*. 2002; 129:5117–5130. [PubMed: 12399304]
30. Charytoniuk DA, Traiffort E, Pinard E, et al. Distribution of bone morphogenetic protein and bone morphogenetic protein receptor transcripts in the rodent nervous system and up-regulation of bone morphogenetic protein receptor type II in hippocampal dentate gyrus in a rat model of global cerebral ischemia. *Neuroscience*. 2000; 100:33–43. [PubMed: 10996456]
31. Samanta J, Kessler JA. Interactions between ID and OLIG proteins mediate the inhibitory effects of BMP4 on oligodendroglial differentiation. *Development*. 2004; 131:4131–4142. [PubMed: 15280210]
32. Samanta J, Alden T, Gobeske K, et al. Noggin protects against ischemic brain injury in rodents. *Stroke*. 2010; 41:357–362. [PubMed: 20019326]
33. Southwell DG, Nicholas CR, Basbaum AI, et al. Interneurons from embryonic development to cell-based therapy. *Science*. 2014; 344:1240622. [PubMed: 24723614]
34. Alagappan D, Lazzarino DA, Felling RJ, et al. Brain injury expands the numbers of neural stem cells and progenitors in the SVZ by enhancing their responsiveness to EGF. *ASN Neuro*. 2009; 1.
35. Buono KD, Goodus MT, Guardia Clausi M, et al. Mechanisms of mouse neural precursor expansion after neonatal hypoxia-ischemia. *J Neurosci*. 2015; 35:8855–8865. [PubMed: 26063918]
36. Dizon ML, Maa T, Kessler JA. The bone morphogenetic protein antagonist noggin protects white matter after perinatal hypoxia-ischemia. *Neurobiol Dis*. 2011; 42:318–326. [PubMed: 21310236]
37. Dummula K, Vinukonda G, Chu P, et al. Bone morphogenetic protein inhibition promotes neurological recovery after intraventricular hemorrhage. *J Neurosci*. 2011; 24:12068–12082.
38. Reid MV, Murray KA, Marsh ED, et al. Delayed myelination in an intrauterine growth retardation model is mediated by oxidative stress upregulating bone morphogenetic protein 4. *J Neuropathol Exp Neurol*. 2012; 71:640–653. [PubMed: 22710965]
39. Izrael M, Zhang P, Kaufman R, et al. Human oligodendrocytes derived from embryonic stem cells: Effect of noggin on phenotypic differentiation *in vitro* and on myelination *in vivo*. *Mol Cell Neurosci*. 2007; 34:310–323. [PubMed: 17196394]

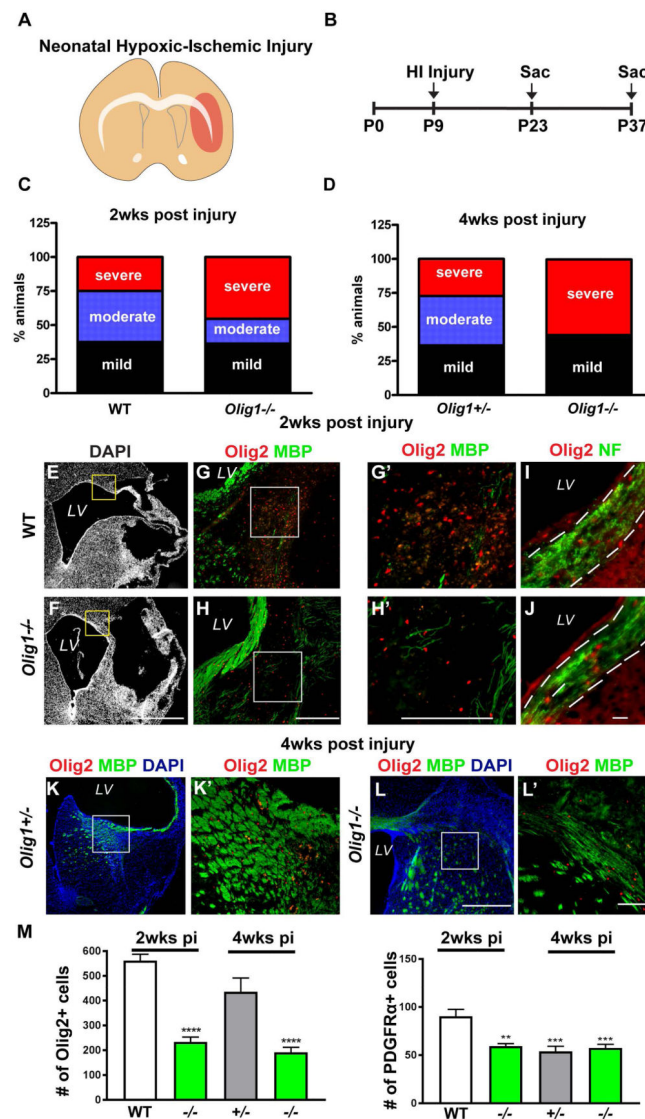


Figure 1. Deficient OPC recruitment and myelination in *Olig1*-null neonatal animals post injury
 (A) Cartoon illustrating neonatal HI injury in the brain. (B) Experimental timeline for neonatal HI injury. (C,D) Analysis of brain injury in wild type and *Olig1*-null animals two and four weeks post HI damage. Most of the brain injury in the *Olig1*-null animals two week post injury was classified as severe (46%), whereas the majority of injury in wild type animals was mild or moderate (38%). At four weeks, 56% of the *Olig1*-null animals showed severe injury compared to 27% of *Olig1*-heterozygous animals. The numbers of mice analyzed for C: wild type n=13; *Olig1*-null n=14 and for D: *Olig1*-heterozygous n = 11; *Olig1*-null n=14. (E,F) Low magnification DAPI image of wild type and *Olig1*-null animals with moderate brain injury. The box represents the region where the images in g–h were taken. (G–H) Merged image of Olig2 (red) and MBP (green) showing lack of myelin and reduced Olig2⁺ cells within the hypercellular lesion. Higher magnification views shown in G'–H'. (I–J) Representative images of Neurofilament (green) and Olig2 (red) immunostaining in the corpus callosum showing intact axons in the area of deficient OPCs.

(K,L) Merged image of Olig2 (red), MBP (green) and DAPI (blue) in *Olig1*-heterozygous and *Olig1*-null animals four weeks post injury. Higher magnification views shown in K'-L'. (M) Cell counts of Olig2+ and PDGFR α + cells in the corpus callosum two and four weeks post injury. Data are mean \pm s.e.m; *n* 4 animals per genotype; **P<0.01; ***P<0.001; ****P<0.0001; one-way ANOVA with Dunnett's multiple comparison test. (F,H,H',L,L') scale bar = 50 μ m, (I-J) scale bar = 20 μ m.

Author Manuscript

Author Manuscript

Author Manuscript

Author Manuscript

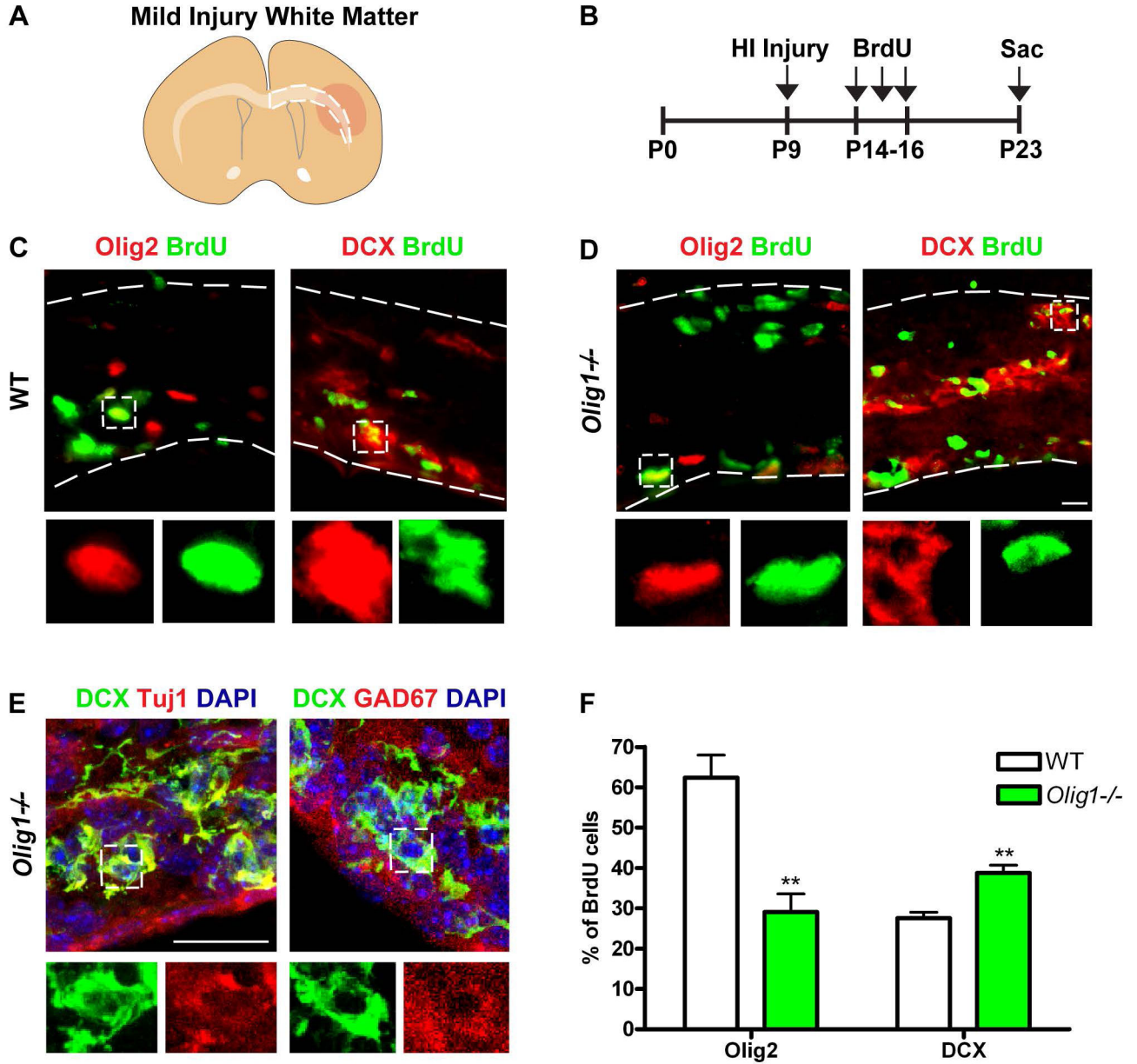


Figure 2. Ectopic production of interneurons and depressed proliferation of OPCs in white matter of *Olig1*-null animals post injury

(A) Cartoon illustrating subcortical white matter in mild neonatal HI injury. (B)

Experimental timeline for BrdU administration following neonatal HI injury. (C–D)

Representative image of DCX (red) or Olig2 (red) and BrdU (green) immunostaining in the subcortical white matter of a wild type and *Olig1*-null animal two weeks post injury. Note the increased number of proliferating DCX-positive cells in the subcortical white matter of an *Olig1*-null animal. (E) Confocal projections showing that DCX (green) colocalizes with cellular Tuj1 (red) and GAD67 (red) in the subcortical white matter of *Olig1*-null animals.

(F) Quantification of the percentage of BrdU cells expressing DCX or Olig2 in the

subcortical white matter of wild type and *Olig1*-null animals. Data are mean \pm s.e.m; $n=3$ animals per genotype; ** $P<0.01$; Student's two-tailed t test. (D,E) scale bar = 20 μ m.

Author Manuscript

Author Manuscript

Author Manuscript

Author Manuscript

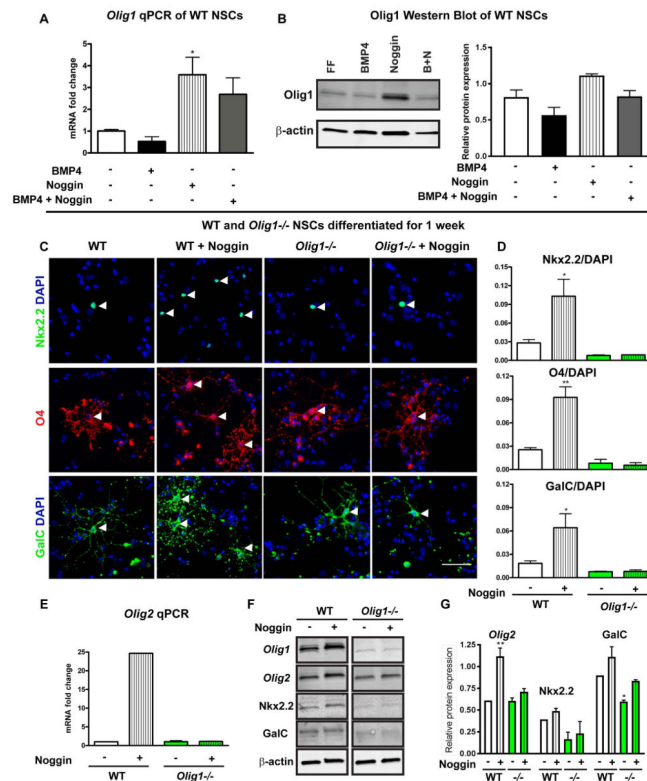


Figure 3. Noggin induction of OPCs from neural stem cells is *Olig1* dependent

(A–B) Quantitative PCR and Western blot from adherent cultures derived from P7 wild type SVZ and cultured in the presence of BMP4, Noggin or BMP4+Noggin for six hours showing that Noggin increased expression of *Olig1* at the mRNA and protein level. (C) Representative images of adherent cultures derived from P7 wild type and *Olig1*-null mouse SVZ, differentiated for seven days in presence or absence of Noggin and stained for Nkx2.2, O4 and GalC. Arrowheads indicate positive cells. (D) Cell counts of Nkx2.2, O4 and GalC in differentiated wild type and *Olig1*-null cultures. (E–G) Quantitative PCR and western blot adherent cultures derived from P7 wild type and *Olig1*-null SVZ, differentiated for seven days in presence or absence of Noggin and assessed for expression of OL markers. Data are mean \pm s.e.m; $n=3$ experiments; * $P<0.05$; ** $P<0.01$; Dunnett's multiple comparison test. (C) scale bar = 50 μ m.

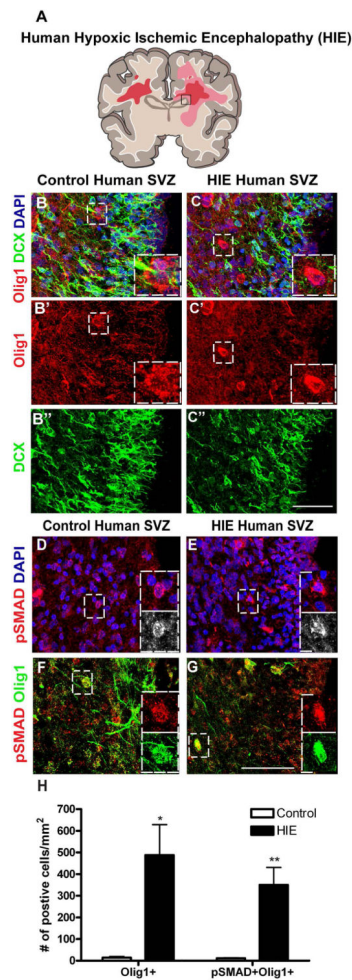


Figure 5. Olig1 overexpression in SVZ progenitors in human HIE

(A) Cartoon illustrating affected white matter areas in human pediatric HIE. The box represents the SVZ region used for analysis. (B–C) Merged confocal projections of DCX (green), Olig1 (red) and DAPI (blue) immunostaining in the human SVZ of control and HIE tissue. Single channel views shown in B', B'', C', C''. In panel C', note the increased number of Olig1+ cells in the HIE SVZ. (D–E) Representative images of pSMAD1/5/8 immunostaining in control and HIE SVZ tissue with DAPI counterstain. Boxes depict positive cells. (F–G) Confocal projections showing colocalization of pSMAD1/5/8 (red) and Olig1 (green) in control and HIE SVZ tissue. Boxes depict double positive cells. (H) Quantification of pSMAD1/5/8 and Olig1 in the SVZ of control and HIE subjects. Data are mean \pm s.e.m; $n = 3$ subjects; * $P < 0.05$; ** $P < 0.01$; Student's two-tailed t test. (C', G) scale bar = 50 μ m.

Table 1

Characteristics of human HIE and control samples

Case #	Diagnosis	Gestational Age	Postconceptional Age at Death	Clinical information
1	HIE	Full term	2 months old	Hypoplastic left heart and diffuse WMI in brain with focal neuron dropout in cerebral and cerebellar cortices
2	HIE	26 wks	5 months old	Failure to thrive, enterocolitis, hypoxemia and ventriculomegaly
3	HIE	37–4/7 wks	6 days old	Therapeutic hypothermia with diffuse WMI
4	Control	31 wks	7 months old	
5	Control	37–3/7 wks	2 days old	Diaphragmatic hernia
6	Control	36–4/7 wks	0 day	Diaphragmatic hernia
7	Control	37–6/7 wks	11 days old	